Active-Disturbance-Rejection-Based Sliding-Mode Current Control for Permanent-Magnet Synchronous Motors

Lizhi Qu, *Member, IEEE*, Wei Qiao, *Fellow, IEEE*, and Liyan Qu, *Senior Member, IEEE*

***Abstract*—To improve the tracking performance of the current controllers of permanent-magnet synchronous motor (PMSM) drive systems that are subject to internal disturbances, such as parameter variations, a novel active-disturbance-rejection-based sliding-mode current control (ADR-SMCC) scheme for PMSM drives is proposed in this article. First, a fast-response SMCC is designed based on the upper bound of the internal disturbance. Then, an extended state observer (ESO) is designed to estimate the internal disturbance in real time without the need for an accurate mathematical model of the PMSM. The parameters of the ESO can be easily designed based on the desired bandwidth of the ESO. The estimated internal disturbance is then used to update the control law of the SMCC in real time. The resulting ADR-SMCC has improved steady-state and transient current tracking performance and enhanced robustness to internal disturbances. The stability of the closed-loop PMSM drive system with the ADR-SMCC is proven by the Lyapunov theory. The ADR-SMCC is validated by experimental results for a 200-W salient-pole PMSM drive system.**

***Index Terms*—Active disturbance rejection control (ADRC), extended state observer (ESO), permanent-magnet synchronous motor (PMSM), sling-mode current control (SMCC).**

I. Introduction

PERMANENT-MAGNET synchronous motors (PMSMs) have been widely employed in industrial applications due to their high reliability, high efficiency, and high power density [1], [2]. The PMSM drives usually adopted a double closed-loop control scheme designed by using the field-oriented control (FOC) technique. The inner current control loop, which affects the performance of the drive system directly, needs precise tracking performance. Due to its simplicity, the traditional linear proportional-integral (PI) control method has been widely applied to design the current controllers for PMSM drives [3]. However, parameter variations or mismatches, which are considered as uncertain internal disturbances in this article, are always present in practical PMSM drives. The performance of the traditional linear PI controller will degrade when the disturbances occur.

To improve the performance of the PMSM drive systems with uncertain disturbances, many current control schemes, such as hysteresis control [4], [5], model predictive control (MPC) [6], [7], and sliding-mode control (SMC) [8]–[15], have been developed for PMSM drives. Among these current control schemes, the hysteresis control provides some advantages, such as simple algorithm implementation, fast current response, and strong robustness to disturbances [5], but it also has some drawbacks, such as variable switching frequencies and large current ripples. Based on a discrete-time model of the PMSM, the MPC can forecast and determine future voltage vectors to optimize a certain cost function, such as the robustness to disturbances [7]. However, precise predictions in the MPCs may need high computational costs, which may limit industrial applications of some MPCs. The SMC method has demonstrated superior tracking performance with simple implementation as compared to the hysteresis control and MPC in different applications [8]–[10]. However, since the disturbances usually vary over large ranges, the robustness of the SMC to disturbances was usually achieved by using a large switching gain, which yielded an undesired chattering problem [8]. To overcome this drawback, combining the SMC with a disturbance observer is an attractive proposition. The disturbance observer estimates the internal disturbance of the system in real time. The estimated disturbance is then used timely to adapt the switching gain of the SMC to mitigate the impact of the disturbance variation on the performance of the SMC [11], [12]. Various disturbance observers combined with SMCs have been designed for the speed and/or current controls of PMSM drives [13]–[15]. However, the design of these disturbance observers still relies on an accurate model of the drive system. Moreover, their parameter designs are complex.

Recently, a new method called active disturbance rejection control (ADRC) [16], [17] has attracted considerable attention due to its intrinsic ability of disturbance rejection and the simple design process without the need for an accurate system model. The ADRC has been applied in motor drives [18]–[20]. In [18], a robust control scheme using three first-order ADRCs was presented for the speed control of induction motor drives without the need for rotor flux estimation, which reduced the

Manuscript received November 7, 2019; revised February 22, 2020; accepted June 7, 2020. Date of publication June 18, 2020; date of current version September 4, 2020. This work was supported in part by the U.S. National Science Foundation under CAREER Award ECCS-1554497 and in part by the Nebraska Public Power District through the Nebraska Center for Energy Sciences Research. Recommended for publication by Associate Editor J. Zhang.
(Corresponding author: Wei Qiao; Liyan Qu.)

Lizhi Qu is with the Toshiba International Corporation, Houston, TX 77041 USA (e-mail: lizhi.qu@huskers.unl.edu).

Wei Qiao and Liyan Qu are with the Power and Energy Systems Laboratory, Department of Electrical and Computer Engineering, University of Nebraska–Lincoln, Lincoln, NE 68588 USA (e-mail: wqiao3@unl.edu; lqu2@unl.edu).

Color versions of one or more of the figures in this article are available online at https://ieeexplore.ieee.org.

Digital Object Identifier 10.1109/TPEL.2020.3003666

computing cost. In [19], an ADRC-based sensorless control scheme for interior PMSM drives was proposed to improve the stiffness of the speed loop by estimating and compensating for the total disturbance of the sensorless drive system. However, the current loop was still designed by using the conventional PI controller. In [20], a hybrid sensorless FOC scheme combining an ADRC-based high-frequency current injection method with another ADRC-based back electromotive force method for the rotor position estimations of PSMSs in low- and high-speed regions, respectively, was presented. The two ADRC-based rotor position estimation methods were integrated into the same current controllers designed by using the simple proportional control method.

This article proposes a novel active-disturbance-rejection-based sliding-model current controller (ADR-SMCC) for FOC-based PMSM drives to improve their disturbance rejection ability as well as steady-state and dynamic current tracking performance. The disturbances considered include PMSM inductance and resistance variations. The ADR-SMCC combines an SMCC with an extended state observer (ESO), which is a core part of the ADRC. The SMCC is designed to achieve fast current tracking performance based on the upper bound of the internal disturbance, which is estimated in real time by the ESO. The design of the ESO does not require an accurate mathematical model of the PMSM. Moreover, the parameters of the ESO can be simply designed based on its desired bandwidth. The control law of the SMCC is then updated in real time by using the upper bound of the disturbance estimated by the ESO in the feedforward path to mitigate the influence of the disturbance on the current tracking performance in both steady-state and transient conditions. Thus, the ADR-SMCC is robust to system disturbances while maintaining fast current tracking performance. The stability of the closed-loop PMSM drive system with the ADR-SMCC is proven by using the Lyapunov theory.

The rest of article is organized as follows. Section II presents the dynamic model of a salient-pole PMSM that considers disturbances and the SMCC design. Section III presents the proposed ESO and ADR-SMCC, the current tracking error dynamic analysis, and the parameter design method for the ESO. Experimental results on a salient-pole PMSM drive system are provided in Section IV to show the superiority of the ADR-SMCC over the conventional PI current controller (PICC), the SMCC, and the disturbance observer-based SMCC (DO-SMCC). Finally, Section V concludes this article.

II. SMCC Design for PMSM Drives

A. Dynamic Model of a Salient-Pole PMSM Considering Disturbances

The current model of a salient-pole PMSM in the *d*–*q* reference frame considering parameter variations is expressed as

$$\begin{cases} pi_{sd} = (v_{sd} - R_{s0}i_{sd} + \omega_{re}L_{q0}i_{sq})/L_{d0} + f_{d_d} \\ pi_{sq} = (v_{sq} - R_{s0}i_{sq} - \omega_{re}L_{d0}i_{sd} - \psi_{m0}\omega_{re})/L_{q0} + f_{d_q} \end{cases} \tag{1}$$

where v_{sd} and v_{sq} are the *d*- and *q*-axis stator voltages, respectively; i_{sd} and i_{sq} are the *d*- and *q*-axis stator currents, respectively; ω_{re} is the rotor electrical angular speed; $p = d/dt$ is the time derivative operator; R_{s0} is the nominal stator armature resistance; L_{d0} and L_{q0} are the nominal *d*- and *q*-axis inductances, respectively; ψ_{m0} is the nominal rotor magnet flux linkage; f_{d_d} and f_{d_q} represent the *d*- and *q*-axis unknown internal disturbances containing the information of parameter variations, respectively, which are defined as follows:

$$\begin{aligned} f_{d_d} &= (-\Delta R_s i_{sd} - \Delta L_d p i_{sd} + \omega_{re}\Delta L_q i_{sq})/L_{d0} \\ f_{d_q} &= (-\Delta R_s i_{sq} - \omega_{re}\Delta L_d i_{sd} - \Delta L_q p i_{sq} - \Delta\psi_m\omega_{re})/L_{q0} \end{aligned} \tag{2}$$

where $\Delta R_s = R_s - R_{s0}$; $\Delta L_d = L_d - L_{d0}$; $\Delta L_q = L_q - L_{q0}$; $\Delta\psi_m = \psi_m - \psi_{m0}$; R_s, L_d, L_q, and ψ_m denote the actual parameter values. In addition, assume that $|\Delta R_s| < a$, $|\Delta L_d| < b$, $|\Delta L_q| < c$, and $|\Delta\psi_m| < d$, where *a*, *b*, *c*, and *d* are the corresponding upper bounds of the parameter variations.

B. SMCC Design for the PMSM

Define the *q*-axis stator current error e_q as follows:

$$e_q = i_{sqr} - i_{sq} \tag{3}$$

where i_{sqr} is the *q*-axis stator current reference. The objective of the SMCC is to control e_q to be zero.

To design the SMCC, the following sliding surface function [15] is chosen due to its simple structure and precise current tracking performance:

$$\sigma_q = e_q + c_q \int e_q \tag{4}$$

where c_q is a positive number that determines the decay rate of the *q*-axis stator current error.

Then, a suitable control law is derived such that σ_q satisfies the following sliding mode condition:

$$\sigma_q\dot{\sigma}_q < 0. \tag{5}$$

If (5) is satisfied, σ_q will approach zero in finite time. To satisfy (5), the control law of the SMCC can be designed as follows to generate the *q*-axis stator voltage reference v_{sqr}:

$$\begin{aligned} v_{sqr} = L_{q0}[&pi_{sqr} + R_{s0}i_{sq}/L_{q0} + \omega_{re}L_{d0}i_{sd}/L_{q0} \\ &+ \psi_{m0}\omega_{re}/L_{q0} + c_q e_q + \eta_q \mathrm{sgn}(\sigma_q)] \end{aligned} \tag{6}$$

where sgn is the sign function and η_q is the *q*-axis switching gain, which guarantees the stability, induces a sliding motion on the sliding surface in finite time, and is defined as follows:

$$\eta_q > \frac{1}{L_{q0}}\left(a\,|i_{sq}| + b\,|\omega_{re}|\,|i_{sd}| + c\,|pi_{sq}| + d\,|\omega_{re}|\right). \tag{7}$$

Then, the sliding mode condition (5) can be proven to be satisfied as follows:

$$\begin{aligned} &\sigma_q\dot{\sigma}_q \\ &= \sigma_q(pi_{sqr} - pi_{sq} + c_q e_q) \\ &= \sigma_q(pi_{sqr} - v_{sq}/L_{q0} + R_{s0}i_q/L_{q0} + \omega_{re}L_{d0}i_{sd}/L_{q0} \\ &\quad + \psi_{m0}\omega_{re}/L_{q0} + \Delta R_s i_{sq}/L_{q0} + \omega_{re}\Delta L_d i_{sd}/L_{q0} \end{aligned}$$

$$\begin{aligned}&+ \Delta L_q p i_{sq}/L_{q0} + \Delta\psi_m\omega_{re}/L_{q0} + c_q e_q)\\
&= -\eta_q\left|\sigma_q\right| + (\Delta R_s i_{sq} + \omega_{re}\Delta L_d i_{sd} + \Delta L_q p i_{sq}\\
&+ \Delta\psi_m\omega_{re})\sigma_q/L_{q0}\\
&\le -\eta_q\left|\sigma_q\right| + (\left|\Delta R_s\right|\left|i_{sq}\right| + \left|\Delta L_d\right|\left|\omega_{re}\right|\left|i_{sd}\right| + \left|\Delta L_q\right|\left|p i_{sq}\right|\\
&+ \left|\Delta\psi_m\right|\left|\omega_{re}\right|)\left|\sigma_q\right|/L_{q0}\\
&\le -\eta_q\left|\sigma_q\right| + (a\left|i_{sq}\right| + b\left|\omega_{re}\right|\left|i_{sd}\right| + c\left|p i_{sq}\right|\\
&+ d\left|\omega_{re}\right|)\left|\sigma_q\right|/L_{q0}\\
&= [-\eta_q + (a\left|i_{sq}\right| + b\left|\omega_{re}\right|\left|i_{sd}\right| + c\left|p i_{sq}\right|\\
&+ d\left|\omega_{re}\right|)/L_{q0}]\left|\sigma_q\right| < 0.\end{aligned} \quad (8)$$

Thus, the closed-loop q-axis current control system is asymptotically stable [21].

The d-axis control voltage v_{sdr} can be derived in a similar way. Consider the current model (1) and define the q-axis stator current tracking error $e_d = i_{sdr} - i_{sd}$ and the d-axis sliding surface function as $\sigma_d = e_d + c_d\int e_d$, where i_{sdr} is the d-axis stator current reference; c_d is a positive number that determines the decay rate of the d-axis stator current error. Then, v_{sdr} can be obtained as follows to satisfy the sliding mode condition $\sigma_d\dot{\sigma}_d < 0$:

$$\begin{aligned}v_{sdr} = L_{d0}[&p i_{sdr} + R_{s0}i_{sd}/L_{d0} - \omega_{re}L_{q0}i_{sq}/L_{d0} + c_d e_d\\
&+ \eta_d\mathrm{sgn}(\sigma_d)]\end{aligned} \quad (9)$$

where η_d is the d-axis switching gain, which guarantees the stability, induces a sliding motion on the sliding surface in finite time, and is defined as follows:

$$\eta_d > \frac{1}{L_{d0}}\left(a\left|i_{sd}\right| + b\left|p i_{sd}\right| + c\left|\omega_{re}\right|\left|i_{sq}\right|\right). \quad (10)$$

III. Proposed ADR-SMCC for PMSM Drives

The SMCC has a certain degree of robustness to the internal disturbance, i.e., parameter variations. To minimize the effect of the chattering problem, a small switching gain is desired for the SMCC. However, to ensure that the SMCC is robust to large disturbances, a large switching gain is desired, which, however, will lead to the undesired chattering problem. An attractive proposition to solve this dilemma is to make the control law of the SMCC adaptive to the disturbance, which is estimated online by a disturbance observer.

A. Proposed ADR-SMCC for the PMSM

An ESO is designed as follows to online estimate the q-axis internal disturbance f_{d_q} that contains the information of the unknown q-axis parameter variations:

$$\begin{cases} e_{sq} = \hat{i}_{sq} - i_{sq}\\ p\hat{i}_{sq} = v_{sq}/L_{q0} - R_{s0}\cdot i_{sq}/L_{q0} - \omega_{re}\cdot L_{d0}\cdot i_{sd}/L_{q0}\\ \qquad -\psi_{m0}\cdot\omega_{re}/L_{q0} + \hat{f}_{d_q} - \beta_{01}e_{sq}\\ p\hat{f}_{d_q} = -\beta_{02}e_{sq}\end{cases} \quad (11)$$

where $\hat{i}_{sq}$ is the estimated q-axis stator current; $\hat{f}_{d_q}$ represents the estimated q-axis internal disturbance; β_{01} and β_{02} are the gains of the ESO.

By taking into account the estimated internal disturbance, a new q-axis control law of the SMCC is designed as follows to generate the new q-axis stator voltage reference v'_{sqr}:

$$\begin{aligned}v'_{sqr} = L_{q0}[&p i_{sqr} + R_{s0}i_{sq}/L_{q0} + \omega_{re}L_{d0}i_{sd}/L_{q0}\\
&+ \psi_{m0}\omega_{re}/L_{q0} + c_q e_q + \eta'_q\mathrm{sgn}(\sigma_q) + \hat{f}_{d_q}]\end{aligned} \quad (12)$$

where η'_q is a positive constant, which is much smaller than the original switching gain η_q expressed by (7) to avoid the large chatting problem; m_q is the compensation gain designed as $m_q = \sigma_q/\dot{\hat{f}}_{d_q} > 0$.

If the bandwidth of the ESO is high enough as compared with the time variation of the internal disturbance, the variation of f_{d_q} is nearly zero during each short sampling period, such as 100–200 μs commonly used for FOC-based PMSM drives, that is, $\dot{f}_{d_q} = 0$ [15]. Define the internal disturbance observation error $\Delta f_{d_q} = f_{d_q} - \hat{f}_{d_q}$. Then

$$\Delta\dot{f}_{d_q} = \dot{f}_{d_q} - \dot{\hat{f}}_{d_q} = -\dot{\hat{f}}_{d_q}. \quad (13)$$

Define the following Lyapunov function:

$$V = \frac{1}{2}{\sigma_q}^2 + \frac{1}{2}m_q{\Delta f_{d_q}}^2. \quad (14)$$

Then, the derivative of V can be derived as follows:

$$\begin{aligned}\dot{V} &= \sigma_q\dot{\sigma}_q + m_q\Delta f_{d_q}\Delta\dot{f}_{d_q}\\
&= \sigma_q(p i_{sqr} - v_{sq}/L_{q0} + R_{s0}i_q/L_{q0} + \omega_{re}L_{d0}i_{sd}/L_{q0}\\
&\quad + \psi_{m0}\omega_{re}/L_{q0} + f_{d_q} + c_q e_q) + m_q\Delta f_{d_q}\Delta\dot{f}_{d_q}\\
&= \sigma_q[f_{d_q} - \hat{f}_{d_q} - \eta'_q\mathrm{sgn}(\sigma_q)] + m_q\Delta f_{d_q}\Delta\dot{f}_{d_q}\\
&\le -\eta'_q\left|\sigma_q\right| + \left(f_{d_q} - \hat{f}_{d_q}\right)\sigma_q + m_q(\hat{f}_{d_q} - f_{d_q})\dot{\hat{f}}_{d_q}\\
&= -\eta'_q\left|\sigma_q\right| < 0.\end{aligned} \quad (15)$$

Thus, the asymptotical stability of the closed-loop q-axis current control is proved. Finally, the q-axis control law of the proposed ADR-SMCC is obtained by combining (11) and (12).

The d-axis control law of the ADR-SMCC can be derived in a similar way as follows:

$$\begin{aligned}v'_{sdr} = L_{d0}[&p i_{sdr} + R_{s0}i_{sd}/L_{d0} - L_{q0}\omega_{re}i_{sq}/L_{d0}\\
&+ c_d e_d + \eta'_d\mathrm{sgn}(\sigma_d) + \hat{f}_{d_d}]\end{aligned} \quad (16)$$

where η'_d is a positive constant, which is much smaller than the original switching gain η_d expressed by (10) to avoid the large chatting problem; $\hat{f}_{d_d}$ represents the estimated d-axis internal disturbance that contains the information of the unknown d-axis parameter variations.

Fig. 1 depicts the block diagram of the plant controlled by the ADR-SMCC scheme, where x stands for d and q, respectively. Fig. 2 depicts the block diagram of the entire FOC scheme for a PMSM drive that uses the proposed ADR-SMCC for the current tracking control, where the PMSM, inverter, space-vector

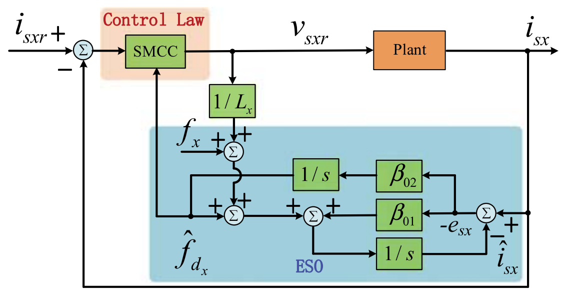

Fig. 1. Block diagram of the plant controlled by the ADR-SMCC scheme.

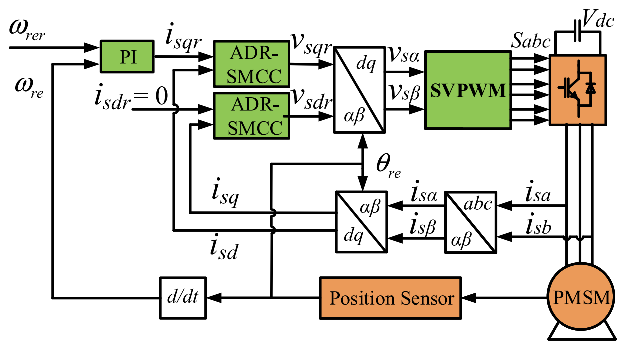

Fig. 2. Block diagram of the ADR-SMCC scheme for a PMSM drive.

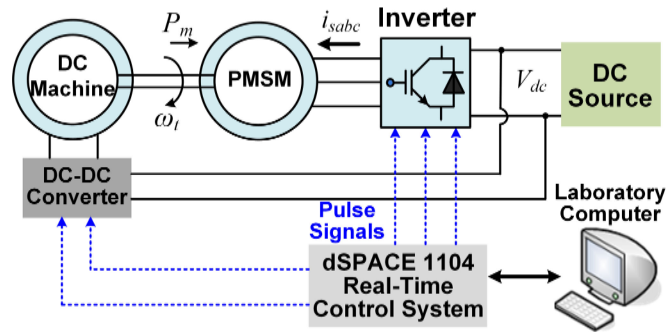

Fig. 3. Block diagram of the experiment system.

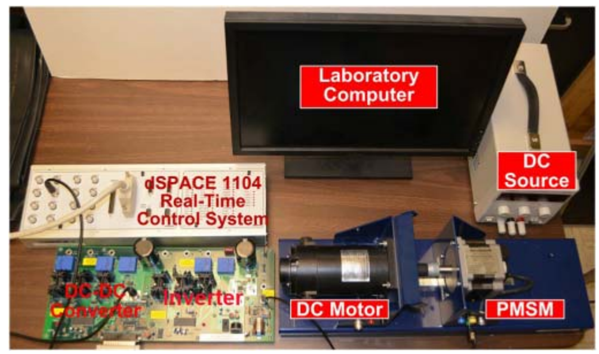

Fig. 4. Hardware setup of the experiment system.

pulsewidth modulation (SVPWM), and coordinate transformation blocks form the plant in Fig. 1. The PMSM is fed by a pulsewidth modulated inverter. The entire control system adopts the commonly used double-loop structure. A PI controller is used for the outer speed loop, which generates the reference i_{sqr} for the torque producing current i_{sq}. The reference of the field current i_{sd} is set to be 0 A. The proposed ADR-SMCC is used for the inner current loop, which generates the desired voltage vector for the pulsewidth modulation (PWM) control of the PMSM inverter. An incremental encoder is used to measure the PMSM rotor position θ_{re} for the coordinate transformation. The rotor speed ω_{re} is obtained by differentiating the rotor position θ_{re}.

B. Stability Analysis and Parameter Design for the ESO

Let $e_{mq} = [\hat{i}_{sq} - i_{sq}, \hat{f}_{d_q} - f_{d_q}]^{\mathrm{T}}$ be the tracking error of the q-axis ESO. According to the q-axis current model in (1) and (11), the error state equation can be derived as

$$\dot{e}_{mq} = A_{mq} e_{mq} \tag{17}$$

where $A_{mq} = \begin{bmatrix} -\beta_{01} & 1 \\ -\beta_{02} & 0 \end{bmatrix}$. Equation (17) shows that the eigenvalues of A_{mq} determine the behavior of the ESO. If and only if $\beta_{02} > 0$, the error dynamics (17) is asymptotically stable.

The parameters of the ESO can be simply designed according to the desired bandwidth of the ESO [22]. Specifically, in this work, the parameters of the ESO are designed such that the matrix A_{mq} has a double eigenvalue λ that is equal to the bandwidth of the ESO. Thus, the following equation should be satisfied:

$$|\lambda E - A_{mq}| = \begin{vmatrix} \lambda + \beta_{01} & -1 \\ \beta_{02} & \lambda \end{vmatrix} = \lambda^2 + \beta_{01}\lambda + \beta_{02} = (\lambda + \omega_0)^2 \tag{18}$$

TABLE I
PARAMETERS OF THE PMSM AND EXPERIMENT SYSTEM

	Parameter	Value	Parameter	Value
PMSM	Rated Speed (rpm)	1500	Rated Power (W)	200
	Rated Load Torque (N·m)	1.5	Nominal Stator Resistance R_{s0} (Ω)	0.235
	Nominal d-axis Inductance L_{d0} (mH)	0.275	Nominal q-axis Inductance L_{q0} (mH)	0.364
	Nominal Moment of Inertia J_0 (kg·m^2)	7e-6	Nominal Flux Linkage ψ_{m0} (V·s)	0.013439
	Voltage Constant K_e (V/rpm)	9.7	# of Pole Pairs n_p	4
Inverter	DC-Bus Voltage (V)	41.75	Switching Frequency (kHz)	10
Control System	Dead time (μs)	1	Sampling Period (μs)	100

where ω_0 is viewed as the bandwidth of the ESO, which should be large enough to ensure that the dynamics of the ESO is sufficiently fast to track the variation of the internal disturbance. Once ω_0 is chosen, the ESO parameters can be determined according to (18) to be $\beta_{01} = 2\omega_0$ and $\beta_{02} = \omega_0{}^2$.

The stability can be analyzed and the parameters can be designed for the d-axis ESO in the same way.

IV. EXPERIMENTAL RESULTS

A. Experiment Setup

Experimental studies are carried out for a 200-W FOC-based salient-pole PMSM drive system to evaluate the proposed ADR-SMCC in comparison with the conventional PICC, the SMCC, and the DO-SMCC [15]. The block diagram and hardware setup of the experiment system are shown in Figs. 3 and 4, respectively. The parameters of the PMSM and experiment system are listed

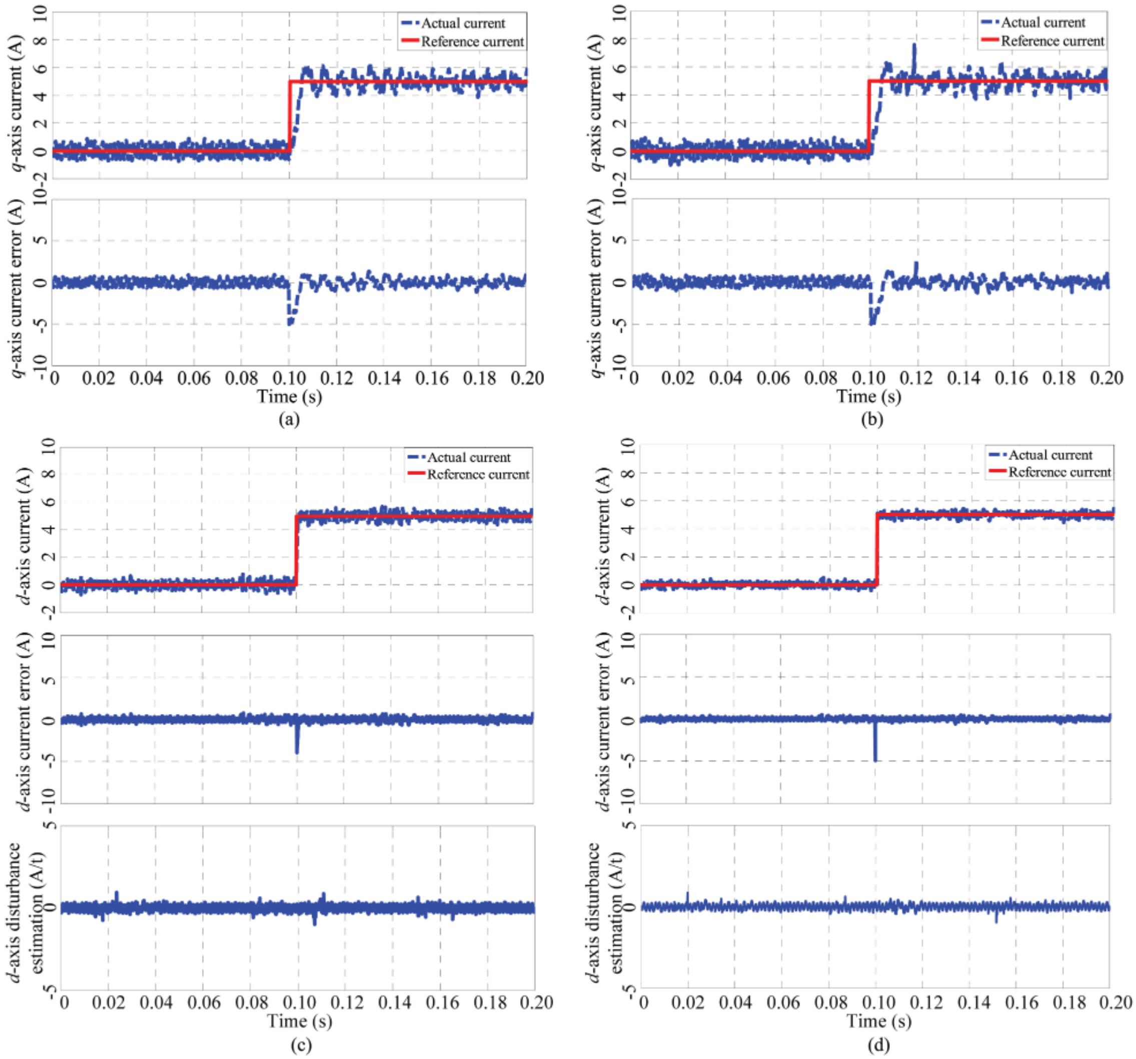

Fig. 5. Experimental results at 1500 r/min with a q-axis current reference step change. (a) PICC. (b) SMCC. (c) DO-SMCC. (d) Proposed ADR-SMCC.

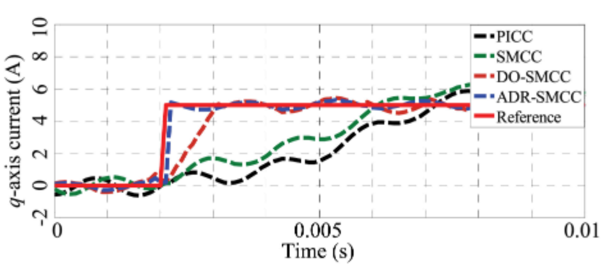

Fig. 6. Comparison of transient responses of the four q-axis current controllers.

TABLE II
PERFORMANCE COMPARISON OF THE FOUR CURRENT CONTROLLERS UNDER A CURRENT REFERENCE STEP CHANGE

Performance metrics		ADR-SMCC	DO-SMCC	SMCC	PICC
Current settling time t_s (ms)	d-axis	0.18	0.90	6.03	7.02
	q-axis	0.15	0.86	4.01	5.18
Current rising time t_r (ms)	d-axis	0.15	0.75	5.54	5.88
	q-axis	0.13	0.66	3.78	4.38
Amplitudes of current tracking errors e_{sd}/e_{sq} (A)	d-axis	0.12/0.12	0.50/0.52	0.65/0.70	0.74/0.85
	q-axis	0.12/0.12	0.55/0.58	0.68/0.73	0.85/0.96

in Table I. The control algorithms are implemented in a dSPACE 1104 real-time control system.

In the experimental studies, the same PI controller with a bandwidth of 285 Hz is used for the speed loops of the FOC systems with the four different current control schemes. The bandwidth of the conventional PICC is chosen as 2000 Hz according to [23] and [24]. The bandwidth of the ESO is designed as 2000 Hz as a tradeoff between current tracking performance and immunity to noise. The SMCC parameter c_q that determines the decay rate of the stator current error is usually between 0 and 1 and is chosen to be 0.1 to achieve fast current tracking performance in this article. The SMCC parameters η_q and η_q' are chosen to be 2 according to (7) and 0.01 according to the definition after (12), respectively. The compensation gain m_q, which only needs to be larger than zero, is chosen to be 0.5 as a tradeoff between steady-state and transient performance. The corresponding parameter settings of the d-axis current controllers of the ADR-SMCC are the same as those of the q-axis current controllers of the ADR-SMCC.

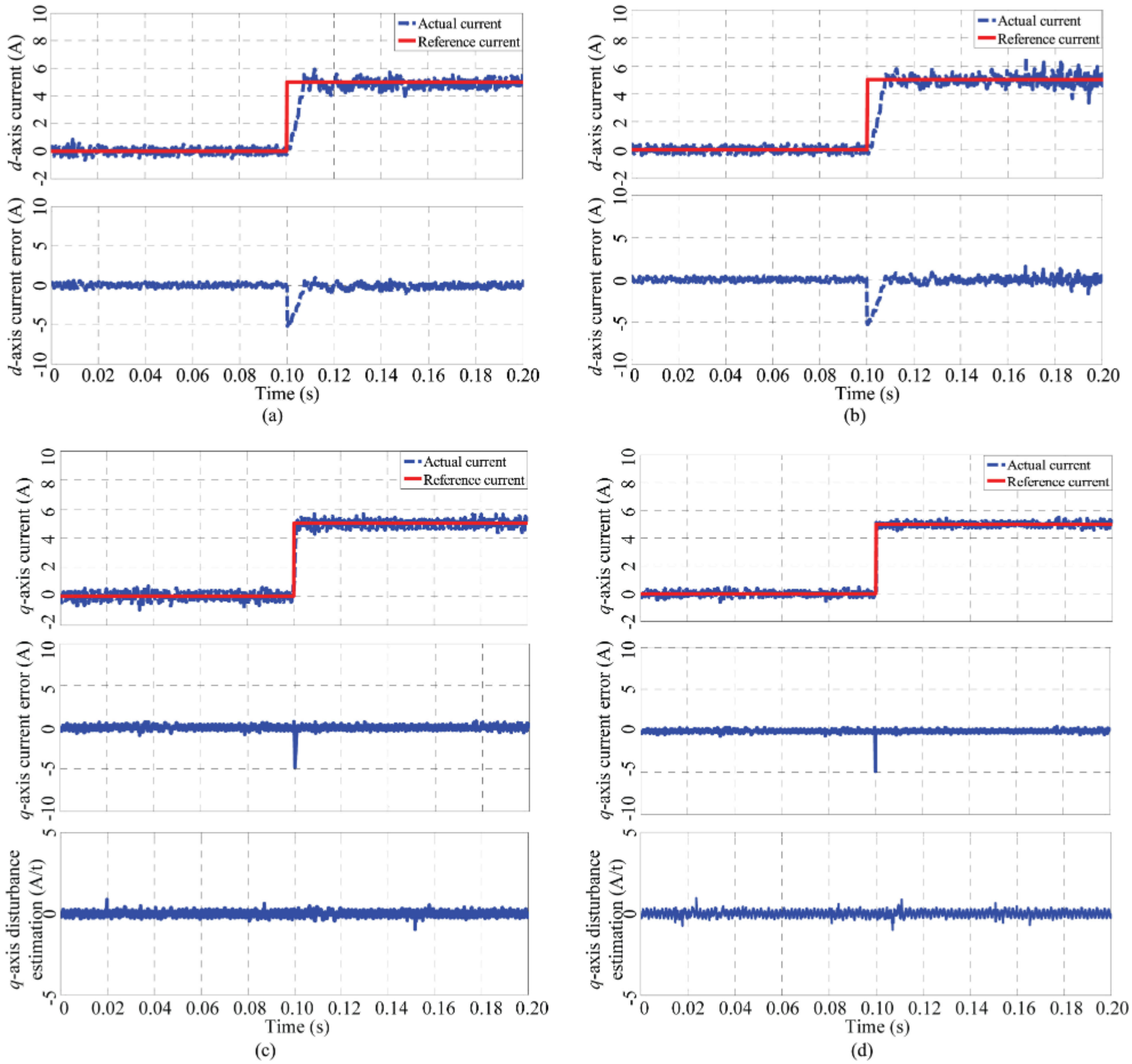

Fig. 7. Experimental results at 1500 r/min with a d-axis current reference step change. (a) PICC. (b) SMCC. (c) DO-SMCC. (d) Proposed ADR-SMCC.

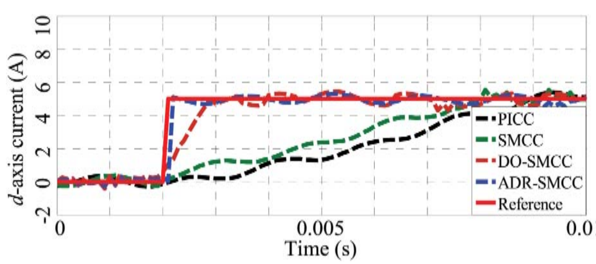

Fig. 8. Comparison of transient responses of the four d-axis current controllers.

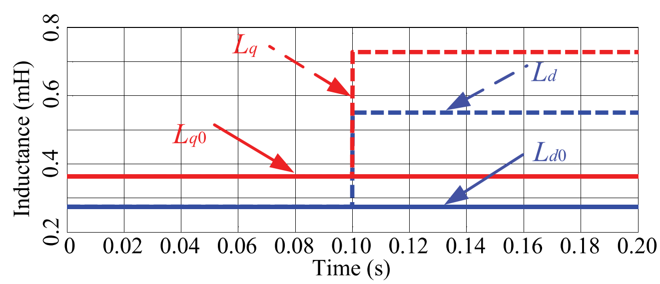

Fig. 9. Mismatch of the d- and q-axis inductances used by the four current controllers.

B. Sudden Current Changes at Constant Speed Without PMSM Parameter Mismatch

In this test, the speed reference is kept constant at 1500 r/min. The q-axis current reference is step changed from 0 to 5 A. Fig. 5 compares the reference and actual q-axis currents and the q-axis current tracking errors of the PMSM with the PICC, the SMCC, the DO-SMCC, and the proposed ADR-SMCC during the test. Fig. 6 compares the detailed transient responses of the

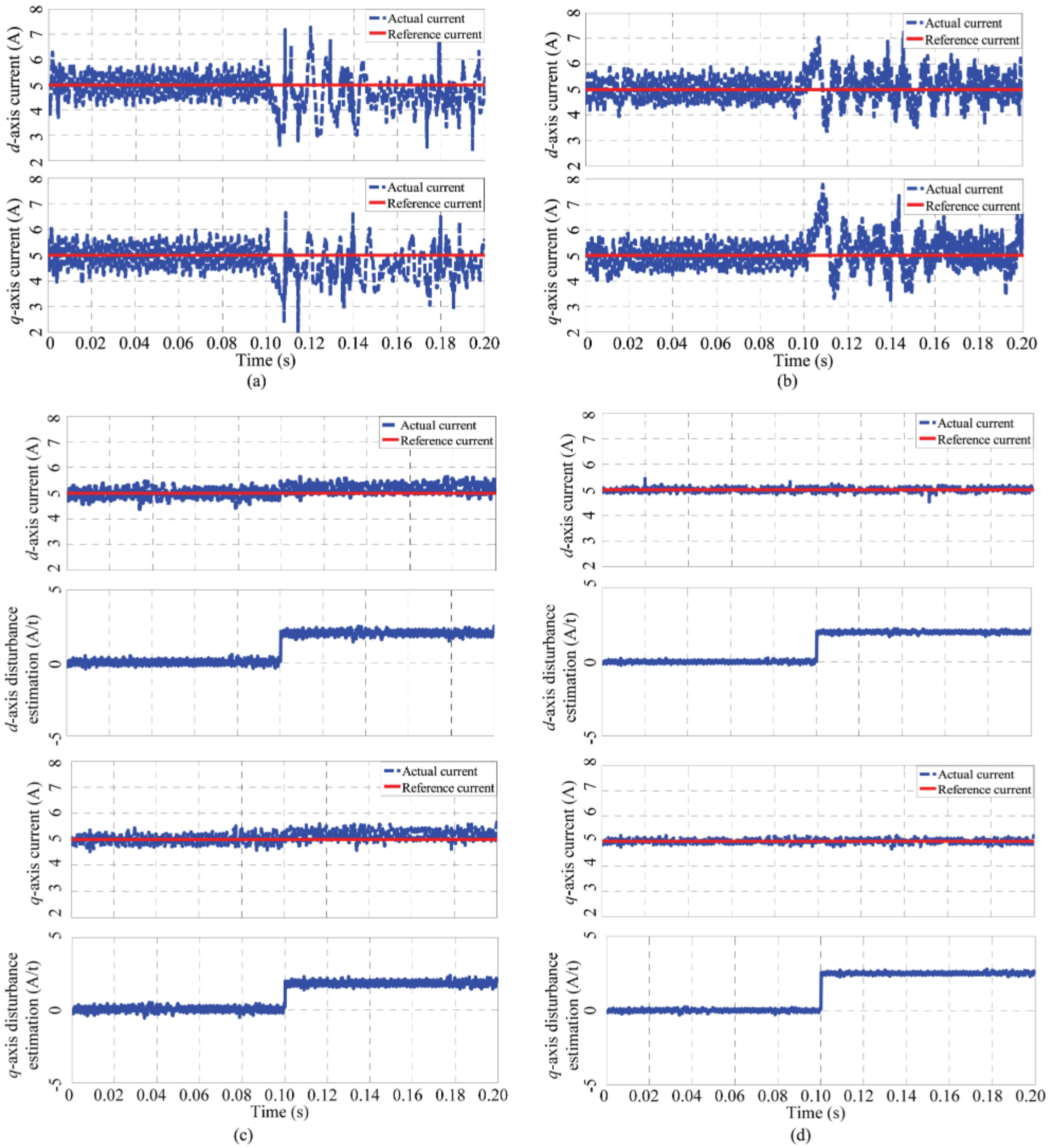

Fig. 10. Experimental results at 1500 r/min with the inductance mismatch. (a) PICC. (b) SMCC. (c) DO-SMCC. (d) Proposed ADR-SMCC.

TABLE III
PERFORMANCE COMPARISON OF THE FOUR CURRENT CONTROLLERS WITH INDUCTANCE MISMATCH

Performance metrics	ADR-SMCC	DO-SMCC	SMCC	PICC
Amplitude of d-axis current tracking error e_{sd} (A) (before/ after inductance mismatch)	0.12 /0.12	0.52 /0.61	0.70 /0.82	0.85 /1.15
Amplitude of q-axis current tracking error e_{sq} (A) (before/ after inductance mismatch	0.12 /0.12	0.58 /0.67	0.73 /0.91	0.96 /1.28

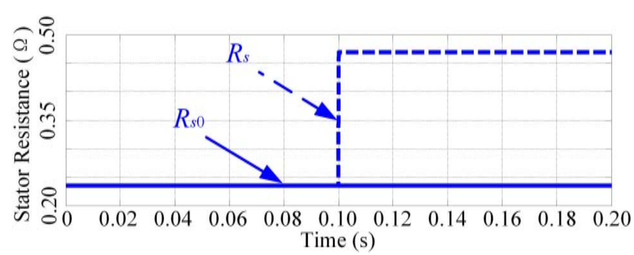

Fig. 11. Mismatch of the stator resistance used by the four current controllers.

four different q-axis current controllers. Table II compares the settling time t_s, rising time t_r, and amplitudes of current tracking error e_{sq} using the four q-axis current controllers after the current reference step change. The test results show that the settling time and rising time of the two observer-based SMCC schemes DO-SMCC and ADR-SMCC after the sudden q-axis current change are much shorter than those of the SMCC and the PICC; the amplitudes of the q-axis current tracking error of the two observer-based SMCC schemes are much smaller than those of

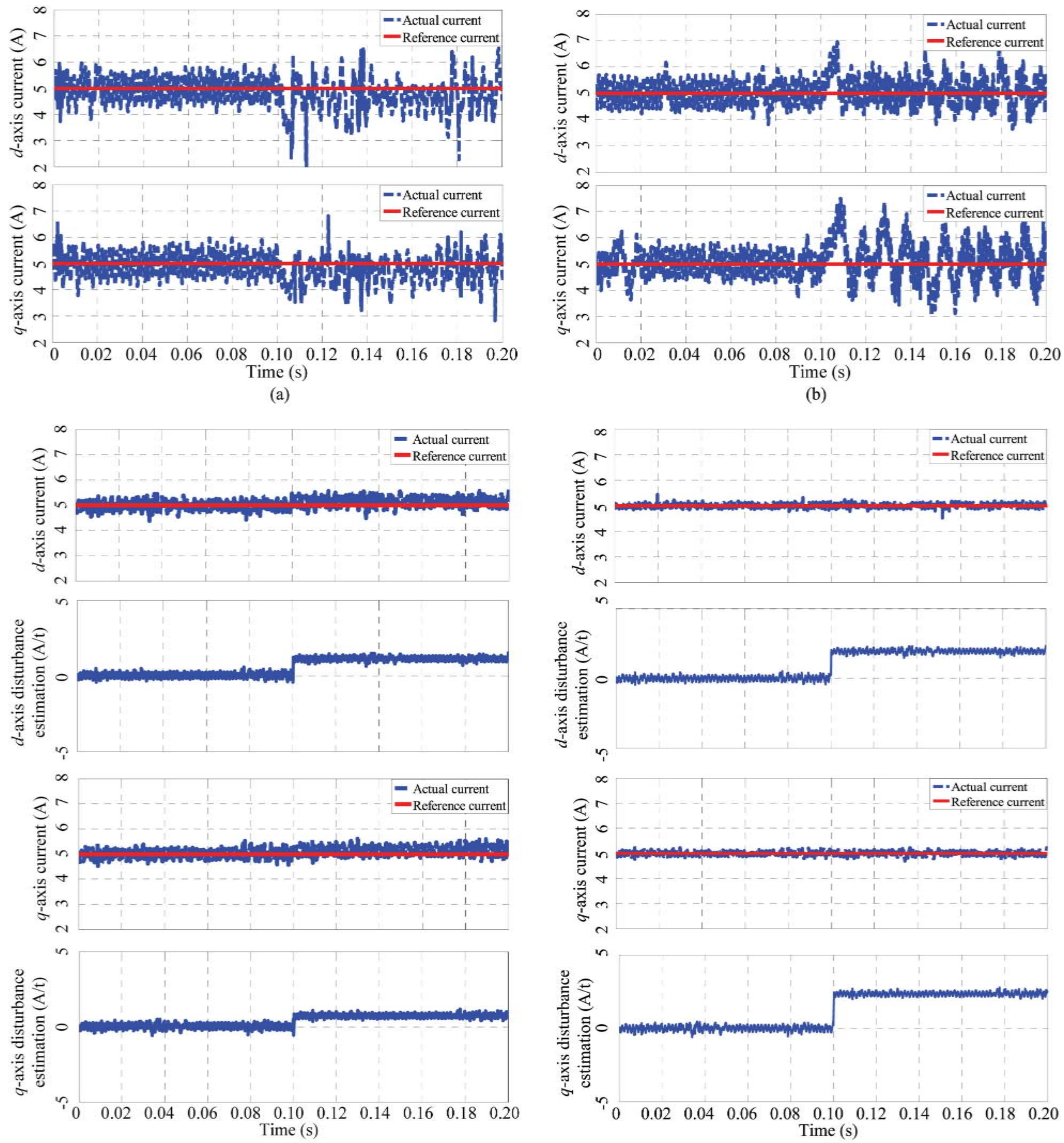

Fig. 12. Experimental results at 1500 r/min with the stator resistance mismatch. (a) PICC. (b) SMCC. (c) DO-SMCC. (d) Proposed ADR-SMCC.

the SMCC and the PICC due to the significant mitigation of the chatting problem. Moreover, with the help of the ESO to properly estimate and compensate for the internal disturbance in (2) in both the steady-state and transient conditions, shown in Fig. 5(d), the transient current tracking performance of the proposed ADR-SMCC is better than that of the DO-SMCC.

Similarly, the d-axis current reference is also step changed from 0 to 5 A. Fig. 7 compares the reference and actual d-axis currents and the d-axis current tracking errors of the PMSM with the PICC, the SMCC, the DO-SMCC, and the proposed ADR-SMCC during the test. Fig. 8 compares the detailed transient responses of the four different d-axis current controllers. Table I also compares the settling time t_s, rising time t_r, and amplitudes of current tracking errors e_{sd} using the four d-axis current controllers after the current reference step change. The test results show that the settling time and rising time of the two observer-based SMCC schemes DO-SMCC and ADR-SMCC after the sudden d-axis current change are much shorter than those of the SMCC and the PICC; the amplitudes of the d-axis current tracking error of the two observer-based SMCC schemes

TABLE IV
PERFORMANCE COMPARISON OF THE FOUR CURRENT CONTROLLERS WITH STATOR RESISTANCE MISMATCH

Performance metrics	ADR-SMCC	DO-SMCC	SMCC	PICC
Amplitude of d-axis current tracking error e_{sd} (A) (before/ after stator resistance mismatch)	0.12 /0.12	0.52 /0.59	0.70 /0.80	0.85 /1.13
Amplitude of q-axis current tracking error e_{sq} (A) (before/ after stator resistance mismatch	0.12 /0.12	0.58 /0.64	0.73 /0.88	0.96 /1.25

are much smaller than those of the SMCC and the PICC due to the significant mitigation of the chatting problem. Moreover, with the help of the ESO to properly estimate and compensate for the internal disturbance in (2) in both the steady-state and transient conditions, shown in Fig. 7(d), the transient current tracking performance of the proposed ADR-SMCC is better than that of the DO-SMCC.

C. Constant Current at Constant Speed With PMSM Parameter Mismatch

In this test, the speed, d-axis, and q-axis current references are kept constant at 1500 r/min, 5 A, and 5 A, respectively. Assume that the d-axis inductance L_d and q-axis inductance L_q used by the four current controllers are mismeasured to be 200% of L_{d0} and L_{q0} from 0.1 s onward, respectively, as shown in Fig. 9. Fig. 10 and Table III compare the current tracking performance of the PMSM using the PICC, the SMCC, the DO-SMCC, and the proposed ADR-SMCC during the test. The results clearly show that the magnitude of the d-axis current tracking error e_{sd} using the proposed ADR-SMCC is much smaller than those using the DO-SMCC, the SMCC, and the PICC. Moreover, with the help of the ESO for estimating and compensating the d-axis internal disturbance in (2) in the ADR-SMCC, shown in Fig. 10(d), the current tracking performance is not affected by the inductance mismatch at all. However, when using the DO-SMCC, the SMCC, or the PICC, the magnitude of the d-axis current tracking error increases significantly when the inductance mismatch occurs. Thus, the ADR-SMCC exhibits a remarkably improved capability of rejecting or robustness to the disturbance (inductance mismatch) compared to the PICC, the SMCC, and the DO-SMCC. Similar results are obtained for the q-axis current controllers, as shown in Fig. 10 and Table III.

In another test, under the same operating condition in Fig. 10, assume that the stator resistance R_s used by the four current controllers are mismeasured to be 200% of R_{s0} from 0.1 s onward, as shown in Fig. 11. Fig. 12 and Table IV compare the current tracking performance of the PMSM using the PICC, the SMCC, the DO-SMCC, and the proposed ADR-SMCC during the test. The results clearly show that the magnitude of the d-axis current tracking error e_{sd} using the ADR-SMCC is much smaller than those using the DO-SMCC, the SMCC, and the PICC. Moreover, with the help of the ESO for estimating and compensating the d-axis internal disturbance in (2) in the ADR-SMCC, shown in Fig. 12(d), the current tracking performance is not affected by the resistance mismatch at all. However, when using the DO-SMCC, the SMCC, or the PICC, the magnitude of the d-axis current tracking error increases significantly when the stator resistance mismatch occurs. Thus, the ADR-SMCC exhibits a remarkably improved robustness to the disturbance (resistance mismatch) compared to the PICC, the SMCC, and the DO-SMCC. Similar results are obtained for the q-axis current controllers, as shown in Fig. 12 and Table IV.

V. CONCLUSION

An ADR-SMCC was proposed for PMSM drive systems to achieve fast dynamic response, precise current tracking performance, and strong robustness to internal disturbances of the system, such as parameter variations or mismatches. First, a fast-response SMCC was designed based on the upper bound of the internal disturbance. Then, an ESO was proposed to online estimate the internal disturbance of the PMSM drive system. Finally, the control law of the SMCC was adapted by compensating the estimated internal disturbance with the stability proven by the Lyapunov theory, leading to an ADR-SMCC with an improved disturbance rejection ability over the SMCC and the DO-SMCC. The experimental results showed that the PMSM drive system using the proposed ADR-based SMCC has a better disturbance rejection capability, smaller current tracking error, and improved dynamic response than that using the conventional PICC, the SMCC, and the DO-SMCC.

REFERENCES

[1] Y. Zhao, C. Wei, Z. Zhang, and W. Qiao, "A review on position/speed sensorless control for permanent-magnet synchronous machine-based wind energy conversion systems," *IEEE J. Emerg. Sel. Topics Power Electron.*, vol. 1, no. 4, pp. 203–216, Dec. 2013.

[2] R. Ni, D. Xu, G. Wang, L. Ding, G. Zhang, and L. Qu, "Maximum efficiency per ampere control of permanent magnet synchronous machines," *IEEE Trans. Ind. Electron.*, vol. 62, no. 4, pp. 2135–2143, Apr. 2015.

[3] R. Sanchis, J. A. Romero, and P. Balaguer, "A simple procedure to design PID controllers in the frequency domain," in *Proc. 35th Annu. Conf. IEEE Ind. Electron. Soc.*, Nov. 2009, pp. 1420–1425.

[4] A. N. Tiwari, P. Agarwal, and S. P. Srivastava, "Performance investigation of modified hysteresis current controller with the permanent magnet synchronous motor drive," *IET Elect. Power Appl.*, vol. 4, no. 2, pp. 101–108, Feb. 2010.

[5] B.-J. Kang and C.-M. Liaw, "A robust hysteresis current-controlled PWM inverter for linear PMSM driven magnetic suspended positioning system," *IEEE Trans. Power Electron.*, vol. 48, no. 5, pp. 956–967, Oct. 2001.

[6] X. Zhang, B. Hou, and Y. Mei, "Deadbeat predictive current control of permanent-magnet synchronous motors with stator current and disturbance observer," *IEEE Trans. Power Electron.*, vol. 32, no. 5, pp. 3818–3834, May 2017.

[7] T. Türker, U. Buyukkeles, and A. F. Bakan, "A robust predictive current controller for PMSM drives," *IEEE Trans. Ind. Electron.*, vol. 63, no. 6, pp. 3906–3914, Jun. 2016.

[8] L. Wang, T. Chai, and L. Zhai, "Neural-network-based terminal sliding mode control of robotic manipulators including actuator dynamics," *IEEE Trans. Ind. Electron.*, vol. 56, no. 9, pp. 3296–3304, Sep. 2009.

[9] V. Q. Leu, H. H. Choi, and J. Jung, "Fuzzy sliding mode speed controller for PM synchronous motors with a load torque observer," *IEEE Trans. Power Electron.*, vol. 27, no. 3, pp. 1530–1539, Mar. 2012.

[10] X. Zhang, L. Sun, K. Zhao, and L. Sun, "Nonlinear speed control for PMSM system using sliding-mode control and disturbance compensation techniques," *IEEE Trans. Power Electron.*, vol. 28, no. 3, pp. 1358–1365, Mar. 2013.

[11] W. H. Chen, J. Yang, S. Li, and L. Guo, "Disturbance-observer-based control and related methods—An overview," *IEEE Trans. Ind. Electron.*, vol. 63, no. 2, pp. 1083–1095, Feb. 2016.

[12] J. Yang, W. Chen, L. Guo, Y. Yan, and S. Li, "Disturbance/uncertainty estimation and attenuation techniques in PMSM drives—A survey," *IEEE Trans. Ind. Electron.*, vol. 64, no. 4, pp. 3273–3285, Apr. 2017.

[13] W. Xu, Y. Jiang, and C. Mu, "Novel composite sliding mode control for PMSM drive system based on disturbance observer," *IEEE Trans. Appl. Supercond.*, vol. 26, no. 7, pp. 1–5, Oct. 2016.
[14] X. Liu, H. Yu, J. Yu, and L. Zhao, "Combined speed and current terminal sliding mode control with nonlinear disturbance observer for PMSM drive," *IEEE Access*, vol. 6, pp. 29594–29601, 2018.
[15] S. -H. Chang, P. -Y. Chen, Y. -H. Ting, and S. -W. Hung, "Robust current control-based sliding mode control with simple uncertainties estimation in permanent magnet synchronous motor drive systems," *IET Elect. Power Appl.*, vol. 4, no. 6, pp. 441–450, Jul. 2010.
[16] J. Han, "From PID to active disturbance rejection control," *IEEE Trans. Ind. Electron.*, vol. 56, no. 3, pp. 900–906, Mar. 2009.
[17] B. Sun and Z. Gao, "A DSP-based active disturbance rejection control design for a 1-kW H-bridge dc-dc power converter," *IEEE Trans. Ind. Electron.*, vol. 52, no. 5, pp. 1271–1277, Oct. 2005.
[18] J. Li, H. Ren, and Y. Zhong, "Robust speed control of induction motor drives using first-order auto-disturbance rejection controllers," *IEEE Trans. Ind. Appl.*, vol. 51, no. 1, pp. 712–720, Jan./Feb. 2015.
[19] G. Zhang, G. Wang, B. Yuan, R. Liu, and D. Xu, "Active disturbance rejection control strategy for signal injection-based sensorless IPMSM drives," *IEEE Trans. Transp. Electrific.*, vol. 4, no. 1, pp. 330–339, Mar. 2018.
[20] B. Du, S. Wu, S. Han, and S. Cui, "Application of linear active disturbance rejection controller for sensorless control of internal permanent-magnet synchronous motor," *IEEE Trans. Ind. Electron.*, vol. 63, no. 5, pp. 3019–3027, May 2016.
[21] V. Utkin, J. Guldner, and J. Shi, *Sliding Mode Control in Electromechanical Systems*. New York, NY, USA: Taylor & Francis, 1999.
[22] Z. Gao, "Scaling and bandwidth-parameterization based controller tuning," in *Proc. Amer. Control Conf.*, Jun. 2003, pp. 4989–4996.
[23] K. J. Astrom and T. Hagglund, *Advanced PID Control*. Durham, NC, USA: Instrum., Syst., Autom. Soc., 2006.
[24] K. J. Astrom and B. Witternmark, *Computer-Controlled Systems: Theory and Design*. Englewood Cliffs, NJ, USA: Prentice-Hall, 1990.

Lizhi Qu (Member, IEEE) received the B.Eng. and M.Eng. degrees in electrical engineering from the Harbin Institute of Technology, Harbin, China, in 2013 and 2015, respectively, and the Ph.D. degree in electrical engineering from the University of Nebraska−Lincoln, Lincoln, NE, USA, in 2019.

In Summer 2018, he was an Electrical Engineering Intern with Ford Motor Company, Dearborn, MI, USA. He is currently a Software Development Engineer II with the Toshiba International Corporation, Houston, TX, USA. His research interests include electric machines and drives and power electronics.

Wei Qiao (Fellow, IEEE) received the B.Eng. and M.Eng. degrees in electrical engineering from Zhejiang University, Hangzhou, China, in 1997 and 2002, respectively, the M.S. degree in high-performance computation for engineered systems from Singapore-MIT Alliance, Singapore, in 2003, and the Ph.D. degree in electrical engineering from the Georgia Institute of Technology, Atlanta, GA, USA, in 2008.

Since August 2008, he has been with the University of Nebraska–Lincoln, Lincoln, NE, USA, where he is currently a Professor with the Department of Electrical and Computer Engineering. He has authored or coauthored more than 250 papers in refereed journals and conference proceedings and holds ten U.S. patents. His research interests include renewable energy systems, smart grids, condition monitoring, power electronics, electric motor drives, energy storage systems, and emerging electrical energy conversion devices.

Dr. Qiao was a recipient of the 2010 U.S. National Science Foundation CAREER Award and the recipient of the 2010 IEEE Industry Applications Society Andrew W. Smith Outstanding Young Member Award. He is an Editor for the IEEE TRANSACTIONS ON ENERGY CONVERSION and an Associate Editor for the IEEE TRANSACTIONS ON POWER ELECTRONICS and the IEEE JOURNAL OF EMERGING AND SELECTED TOPICS IN POWER ELECTRONICS.

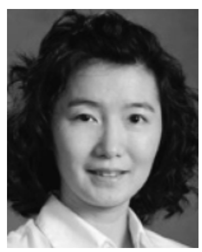

Liyan Qu (Senior Member, IEEE) received the B.Eng. (with the highest distinction) and M.Eng. degrees from Zhejiang University, Hangzhou, China, in 1999 and 2002, respectively, and the Ph.D. degree from the University of Illinois at Urbana–Champaign, Champaign, IL, USA, in 2007, all in electrical engineering.

From 2007 to 2009, she was an Application Engineer with Ansoft Corporation, Irvine, CA, USA. Since January 2010, she has been with the University of Nebraska−Lincoln, Lincoln, NE, USA, where she is currently an Associate Professor with the Department of Electrical and Computer Engineering. Her research interests include energy efficiency, renewable energy, numerical analysis and computer-aided design of electric machinery and power electronic devices, dynamics and control of electric machinery, and magnetic devices.

Dr. Qu was a recipient of the 2016 U.S. National Science Foundation CAREER Award.